Oncology and Translational Medicine
DOI 10.1007/s10330-018-0272-2
June 2018, Vol. 4, No. 3, P108–P115

ORIGINAL ARTICLE

Comparison of computed tomography and magnetic resonance imaging for the detection of mandibular condylar osteochondroma*

Molun Shen[1, 3], Ling Zhu[2], Hongbo Yu[1], Lei Zhang[1], Xudong Wang[1](✉)

[1] Department of Oral and Craniomaxillofacial Surgery, Shanghai Ninth People's Hospital, Shanghai Jiao Tong University School of Medicine, Shanghai Key Laboratory of Stomatology, Shanghai 200011, China
[2] Department of Oral Radiology, Shanghai Ninth People's Hospital, Shanghai Jiao Tong University School of Medicine, Shanghai 200011, China
[3] Department of Oral and Maxillofacial Surgery, Hefei Stomatological Hospital, Hefei 230001, China

Abstract

Objective The purpose of this study was to compare computed tomography (CT) and magnetic resonance imaging (MRI) for the detection of mandibular condylar osteochondroma.

Methods Preoperative CT and MRI of 33 patients with unilateral condylar osteochondroma were reviewed. The morphology, location, continuity with the parent bone, cartilage cap, perichondrium of tumors, and changes in soft and hard tissues adjacent to the lesions were investigated by two reviewers. Data were analyzed using McNemar test. A P value < 0.05 was considered significant.

Results Among the 33 condylar osteochondromas, 11 were of the diffuse type, 10 were of the sessile type, and 12 were of the pedunculated type. Continuity with the cortex and marrow of the host condyle was observed on both CT and MRI. Both modalities had identical detection rates of surface reconstruction of the temporal bone joint, condylar dislocation, and pseudarthrosis formation. However, MRI showed significantly higher detection rates of the cartilage cap and perichondrium than CT (P < 0.05). Furthermore, MRI showed ipsilateral and contralateral temporo-mandibular joint (TMJ) disc displacement in 4 cases and 6 cases, respectively, and ipsilateral and contralateral TMJ effusion in 20 cases and 14 cases, respectively.

Conclusion CT can intuitively display the morphology and spatial location of condylar osteochondromas through three-dimensional reconstruction. MRI may be superior to CT in the detection of cartilage cap, perichondrium of the condylar osteochondroma, and changes in the TMJ and adjacent soft tissues.

Received: 14 April 2018
Revised: 5 May 2018
Accepted: 16 May 2018

Key words: mandibular condyle; osteochondroma; computed tomography (CT); magnetic resonance imaging (MRI)

Osteochondroma is the most-common benign tumor of long bones, but rarely occurs in the mandibular condyle [1]. The typical imaging features of osteochondroma are continuity with the cortex and marrow of the parent bones and a hyaline cartilage cap [2]. Computed tomography (CT) is the most-commonly used imaging modality for condylar osteochondroma: It clearly shows the characteristic continuity of the bone cortex and marrow of the tumor with the corresponding host condylar structures, but poorly demonstrates any uncalcified cartilage cap [3]. In comparison, magnetic resonance imaging (MRI) can directly display the cartilage cap covering the surface of osteochondromas due to its special cartilage signals and plays an important role in the diagnosis of the temporo-mandibular joint (TMJ) disorders [4].

In recent years, with the application of emerging technologies such as endoscopy and navigation, surgical skills for the treatment of condylar osteochondroma have greatly improved [5-7]. However, research progress on diagnostic imaging for this tumor has been slow. MRI studies of mandibular condylar osteochondromas are rarely reported in the literature, and no study has thus far

✉ Correspondence to: Xudong Wang. Email: xudongwang70@hotmail.com
* Supported by Shanghai Municipal Education Commission-Gaofeng Clinical Medicine Grant (No. 20152225); and Shanghai Hospital Development Center Research Grant (No. SHDC12013103)
© 2018 Huazhong University of Science and Technology

compared the efficacy of CT and MRI for its detection. Therefore, in this retrospective study, we analyzed the imaging data of 33 patients with condylar osteochondroma to compare the efficacy of CT and MRI for the detection of various characteristics of this rare disease.

Materials and Methods

Patients

From August 2009 to November 2016, 39 patients with unilateral mandibular condylar osteochondroma underwent surgical treatment at the Department of Oral and Craniomaxillofacial Surgery, Shanghai Ninth People's Hospital, Shanghai Jiao Tong University School of Medicine. Six patients were excluded from our study because their preoperative CT or MR images were not available for review. Finally, 33 patients (6 men and 27 women) were included in this retrospective study. The enrolled patients had a mean age of 27.9 years (range, 17–56 years). The mandibular condylar osteochondroma was located in the left condyle in 14 cases and the right condyle in 19 cases. The final diagnosis of osteochondroma was confirmed by postoperative histopathological examination in all cases.

CT and MRI technique

Preoperative CT and MR images were obtained for all enrolled patients. Thin-cut (1.25 mm) spiral CT [LightSpeed 16 (GE, UK)] was performed with a matrix of 512 × 512 from the calvaria to the hyoid level in each patient. All patients underwent multiplanar reconstruction and volume rendering. The CT images were observed in both bone and soft-tissue windows.

MRI was performed using a 1.5-T unit [Signa Excite TwinSpeed (GE, USA)], with 6 × 8 cm special TMJ surface coils and spin-echo sequences. Proton density-weighted images (PDWI) were obtained in the oblique sagittal mouth-closing position [repetition time/echo time (TR/TE) = 1500.0–1820.0/20.2–20.8 ms, field-of-view (FOV)= 12 cm, slice thickness = 2 mm, matrix = 512 × 512] and the coronal mouth-closing position (TR/TE = 1840.0–2200.0/20.9–21.5 ms, FOV = 12 cm, slice thickness = 1.5 mm, matrix = 512 × 512). T2-weighted images (T2WI) were obtained in the oblique sagittal mouth-opening position (TR/TE = 3160.0–4000.0/81.0–83.2 ms, FOV = 12 cm, slice thickness = 2 mm, matrix = 512 × 512).

Image analysis

The preoperative CT and MR images of all patients were reviewed by a radiologist and a specialist in oral and maxillofacial surgery together. The two reviewers were blinded to the patients' clinical and histopathological information. Reviewer 1 (L.Z.) has > 15 years of oral radiology experience, and reviewer 2 (M.L.S.) has > 10 years of craniomaxillofacial surgery experience with 6 months of training in musculoskeletal radiology. The reviewers evaluated the CT images of each patient first and then the MR images. The morphology, location, continuity with the parent condyle, cartilage cap, and perichondrium of the tumors were analyzed. In addition, the adjacent soft and hard tissues such as the condyle, temporal articular surface, TMJ articular disc, articular cavity, and lateral pterygoid muscle were examined. The thicknesses of the cartilage caps on CT and MR images were measured using a standardized technique proposed by Bernard SA *et al* [8]. When the two reviewers' results were discordant, a third specialist performed a blinded, independent judgment.

Statistical analysis

All data were analyzed using the SPSS17.0 software package (IBM, USA). The McNemar test was used to analyze differences in detection rates of various pathological features and changes in adjacent tissues between CT and MRI. P values < 0.05 were considered statistically significant.

Results

Morphology and location of the condylar osteochondroma

Both CT and MRI clearly displayed the morphology and location of the condylar osteochondromas. However, the spatial position and morphology of the tumor was more innately portrayed by three-dimensional reconstruction of CT images than by MR images (Fig. 1C, Fig. 2C, Fig. 3C). Among the 33 condylar osteochondromas, 11 were of the diffuse type, 10 were of the sessile type, and 12 were of the pedunculated type (Table 1). The diffuse type showed a generally enlarged condyle without obvious boundaries between the tumor and the host condyle (Fig. 1). The sessile and pedunculated osteochondromas manifested exostoses connected with the surface of the condyles through wide bases (Fig. 2) and narrow stalks (Fig. 3), respectively. CT showed that the peripheral density of the tumor was higher than the density at the center, and the internal density was heterogeneous with scattered irregular calcification. MRI showed that the peripheral cortical bone of the tumor was rough with low-signal intensity on PDWI and T2WI. The internal bone marrow showed a moderate, high, or mixed signal on PDWI and T2WI.

In all patients with the diffuse type of osteochondroma, diffuse enlargement of the entire condyle was observed (11/11, 100.0%). Most of the sessile osteochondromas occurred at the anterior or anterior-medial surface of the condyle (5/10, 50.0%). The pedunculated osteochondromas were mostly located on the medial-

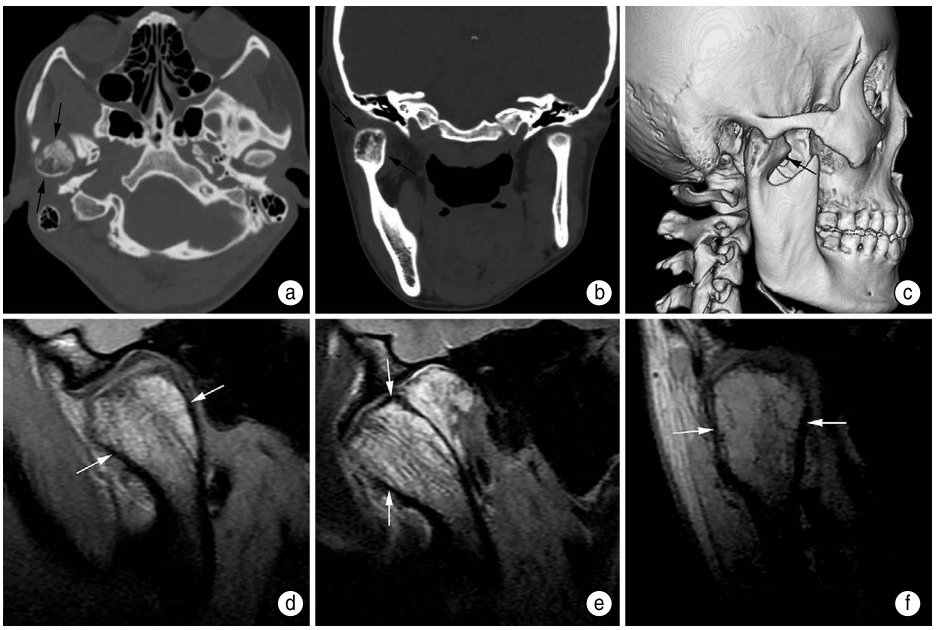

Fig. 1 Osteochondroma of the right condyle in a 27-year-old female patient (arrows). (a) Axial CT showed an enlarged right condyle with heterogeneous density and uneven surface; (b) Coronal CT presented a generally enlarged mass with a spherical shape and without obvious boundary between the lesion and the right condyle; (c) 3D-CT imaging showed a diffused bony outgrowth and significantly elongated ramus; (d) Oblique sagittal PDWI in closed mouth position showed a diffusely enlarged condyle with mixed signal intensity and uneven surface. The posterior belt of articular disc was located above the condyle; (e) Oblique sagittal T2WI in open mouth position showed a long T2 signal in the right articular upper cavity. The middle belt of articular disc was located at the top of the condyle; (f) Coronal PDWI in closed mouth position demonstrated a generally enlarged right condyle with moderate signal intensity.

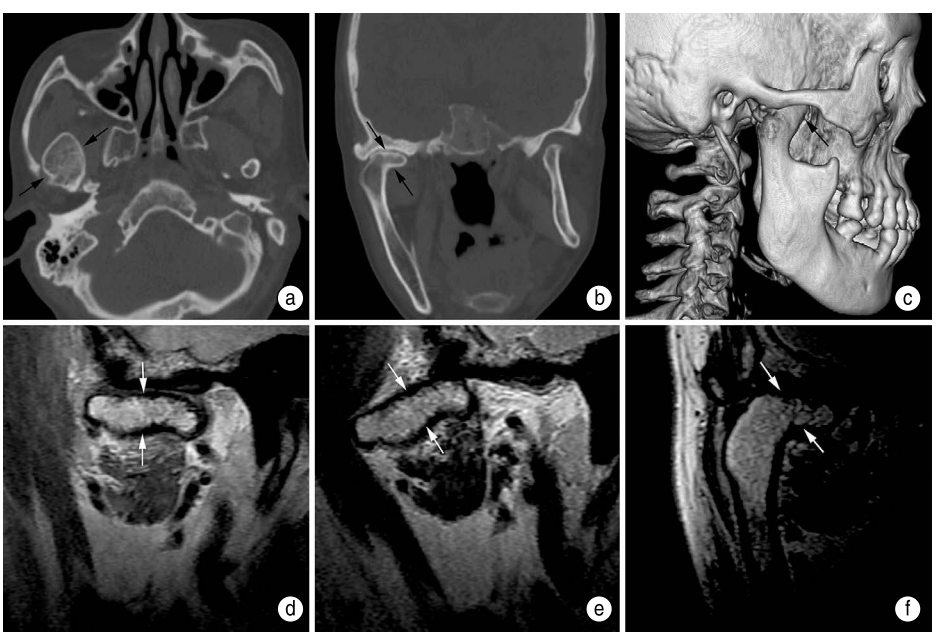

Fig. 2 Osteochondroma of the right condyle in a 56-year-old female patient (arrows). (a) Axial CT showed a bony exostosis arose from the medial area around the right condyle; (b) Coronal CT demonstrated a bony mass located on the medial-superior aspect of the right condyle with well defined border continuous with the parent condylar cortex and medulla; (b) 3D-CT imaging presented a sessile exostosis protruding from the medial-superior aspect of the right condyle. The affected condyle dislocated forward from the glenoid fossa; (d) Oblique sagittal PDWI in closed mouth position showed a high signal exostosis on the medial aspect of the right condyle; (e) Oblique sagittal T2WI in open mouth position showed a high signal exostosis with low signal rim; (f) Coronal PDWI in closed mouth position demonstrated a sessile tumor was located on the medial-superior aspect of the right condyle and was continuous with the underlying condylar cortex and marrow.

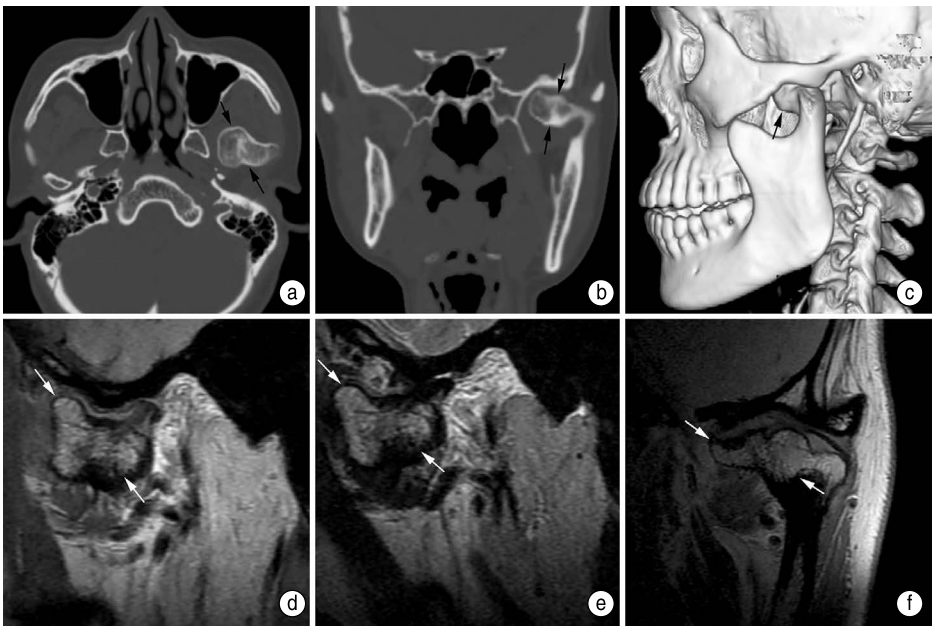

Fig. 3 Osteochondroma of the left condyle in a 32-year-old female patient (arrows). (a) Axial CT showed a bony exostosis arose from the medial area around the left condyle; (b) Coronal CT demonstrated a pedunculated mass located on the medial-superior aspect of the left condyle; (c) 3D-CT imaging showed the left condyle dislocated from the glenoid fossa; (d) Oblique sagittal PDWI in closed mouth position showed a bony tumor on the left condylar anterior-superior edge with mixed signal intensity and the posterior belt of articular disc was located above the condyle; (e) Oblique sagittal T2WI in open mouth position showed there was no change of the relationship of the disc with the condyle when opening mouth with long T2 signal in the articular cavity; (f) Coronal PDWI in closed mouth position demonstrated a pedunculated tumor was located on the medial-superior aspect of the left condyle and was continuous with the underlying condylar cortex and marrow.

superior surface of the condyle (7/12, 58.3%) (Table 1). The condylar osteochondromas presented in varying shapes including spherical (11 cases), hemispherical (4 cases), triangular (4 cases), rectangular (4 cases), beak-like (3 cases), pseudopodia (2 cases), thorn (2 cases), oval (1 case), lip-like (1 case), and cauliflower (1 case).

Table 1 Presenting tumor location surrounding the condyle in 33 cases of condylar osteochondroma

Tumor location	Tumor type (*n*, %)		
	Pedunculated	Sessile	Diffuse
Generally enlarged	0	0	11 (100.0%)
Top	0	1 (10.0%)	0
Posterior-superior	1 (8.3%)	0	0
Simple medial	1 (8.3%)	0	0
Medial-superior	7 (58.3%)	1 (10.0%)	0
Anterior	0	3 (30.0%)	0
Anterior-medial	1 (8.3%)	2 (20.0%)	0
Anterior-superior	1 (8.3%)	1 (10.0%)	0
Lateral-anterior	1 (8.3%)	1 (10.0%)	0
Lateral-posterior	0	1 (10.0%)	0
Total	12 (100.0%)	10 (100.0%)	11 (100.0%)

Detection of various characteristics of condylar osteochondroma on CT and MRI

In all cases, CT and MRI showed the characteristic continuity of the bone cortex and marrow of the osteochondroma with the corresponding host condylar structures (Table 2). The detection rates of the cartilage cap on CT (12 cases, 36.4%) was significantly lower than that on MRI (21 cases, 63.6%) ($P < 0.05$, Table 2). In 12 cases, the thickness of the cartilage caps measured on CT ranged from 2.7 mm to 8.8 mm, with an average of 5.4 mm. The density of the cartilage cap was slightly higher than that of the masticatory muscles. On MRI, the cartilage cap thicknesses in 21 cases ranged from 3.0 mm to 8.5 mm, with an average of 4.6 mm. The cartilage caps showed high-signal or mixed-signal intensity on PDWI and T2WI. The shapes of the cartilage caps were cauliflower-like or irregular and massive.

The detection rates of the perichondrium of the osteochondromas were significantly lower by CT (2 cases, 6.1%) than by MRI (15 cases, 45.5%) ($P < 0.05$, Table 2). On PDWI and T2WI, the perichondrium showed a thin layer of fibrous rings with low-signal intensity around the surface of the cartilage cap. On CT, the density of the perichondrium was slightly lower than that of the masticatory muscles.

Table 2 Comparison of CT and MRI for the detection of various characteristics in 33 cases of condylar osteochondroma

Characteristics	CT		MRI		*P*
	n	%	*n*	%	
Continuity with the parent condyle	33	100.0	33	100.0	/
Cartilage cap	12	36.4	21	63.6	0.004
Perichondrium	2	6.1	15	45.5	0.001
Compressive reconstruction of the temporal bone articular surface	8	24.2	8	24.2	/
Condylar dislocation	10	30.3	10	30.3	/
Pseudojoint	12	36.4	12	36.4	/
Fatty degeneration of the affected lateral pterygoid muscle	3	9.1	8	24.2	0.063
Disc displacement at the affected side	/	/	4	12.1	/
Disc displacement at the contralateral side	/	/	6	18.2	/
Joint effusion at the affected side	/	/	20	60.6	/
Joint effusion at the contralateral side	/	/	14	42.4	/

Detection of the changes in adjacent tissues on CT versus MRI

The results of CT and MRI were consistent with regard to the detection rates of the changes of the affected temporal articular surface, condylar dislocation, and pseudojoint (Table 2). The temporal articular surfaces were flattened due to compression by the tumors in 8 cases (24.2%). The affected condyles were dislocated from the glenoid fossa in 10 cases (30.3%; 5 cases of downward dislocations, 4 cases of forward dislocations, 1 case of lateral displacement). In 10 cases of condylar dislocations, all the osteochondromas occurred at the superior areas around the affected condyle, such as the medial-superior aspect (7 cases, Fig. 2 and 3), the anterior-superior aspect (2 cases), and the top (1 case). In 12 cases (36.4%), the tumor formed a pseudojoint under the anterior joint eminence or middle-skull base.

The detection rates of the affected lateral pterygoid muscle atrophy and fatty degeneration by CT and MRI were 9.1% (3 cases) and 24.2% (8 cases), respectively, with no statistically significant difference ($P > 0.05$, Table 2). CT showed that the affected lateral pterygoid muscle density decreased heterogeneously. MRI showed that the affected lateral pterygoid muscle contained dispersed streaky or patchy high-signal intensities on PDWI and T2WI.

Changes in the affected and contralateral TMJ

CT did not show TMJ articular disc and joint effusion. However, MRI clearly showed disc displacement in the TMJ (Table 2). Four patients (12.1%) had a disc displacement in the affected side (2 cases of irreversible anterior displacement, 1 case of reversible anterior displacement, and 1 case of medial displacement). Six cases (18.2%) had a disc displacement in the contralateral TMJ (3 cases of irreversible anterior disc displacement, 1 case of reversible anterior displacement, 1 case of reversible medial-anterior displacement, and 1 case of irreversible lateral-anterior displacement). Joint effusion was clearly observed on MR images (Fig. 1, Fig. 3, Table 2). Twenty cases (60.6%) of the affected TMJ and 14 cases (42.4%) of the contralateral TMJ had joint effusions presenting as long T2 signals.

Discussion

Condylar osteochondroma usually grows slowly and presents with similar signs and symptoms as TMJ disorders; therefore, it may be misdiagnosed in the early stages [1, 9]. CT is the most-commonly used imaging modality that yields clear bone-tissue images. Through three-dimensional reconstruction of CT images, the position and morphology of the tumor can be innately observed, and the connection between the tumor and the mandibular condyle and glenoid fossa can be clearly visualized [10]. MRI can clearly illustrate the continuity of the osteochondroma and the parent bone as well as the connection between the tumor and its surrounding soft and hard tissues from the multi-planner views. The existence and thickness of the cartilage cap of the tumor can be directly observed by the special cartilage signal on MR images [2, 4]. However, the MRI findings of condylar osteochondroma have thus far only been mentioned in a few case reports, and the literature lacks studies with a large sample size[11–12].

Osteochondromas usually represent pedunculated or sessile exophytic bony protrusions attached to the metaphyseal region of long bones, which are also known as osteocartilagenous exostosis. The sessile and pedunculated tumors are connected with the host bones

through wide bases and narrow stalks, respectively [2]. However, in addition to exogenous excrescence, condylar osteochondromas could manifest with a diffuse growth pattern involving the entire condyle [10–11, 13–14]. In our study, 11 of the 33 tumors were of the diffuse type, with the overall shape of the affected condylar increasing as compared to the contralateral side. Due to the absence of an obvious boundary between the tumor and the host condyle, the diffuse osteochondroma was difficult to differentiate from condylar hyperplasia.

Stress in areas of the tendinous insertion, where the cells with cartilaginous potential accumulate focally, is a possible factor for osteochondroma formation [15]. This possibility is supported by some early studies that showed that most condylar osteochondromas occurred at the anterior-medial surface of the condyle at the attachment of the pterygoid muscle [13]. However, in recent years, studies found that the lesions could be located at different sites encircling the condyle, such as the lateral, anterior-lateral, anterior, superior, and posterior aspect of the condyle [10, 14], which questions the possibility of stress as a factor for osteochondroma formation. In addition, this study showed that the condylar osteochondroma could grow around different parts of the condyle. Although the condylar medial surfaces (including the simple medial, medial-superior, anterior-medial aspects) were the main sites of tumor growth, these aspects constituted only 36.4% of all cases (12/33; Table 1). The tumor also occurred in the top, posterior-superior, anterior, anterior-superior, lateral-anterior, and lateral-posterior surface of the condyle. Zhang *et al*. argued that osteochondromas might occur at any site of the condyle as long as continuous local stimulation persisted [14], which is in line with our findings. Both CT and MRI have multiple-planar imaging capabilities. As such, both modalities can present the growth position and morphology of osteochondroma from several different perspectives. However, CT images can be reconstructed to obtain a three-dimensional digital model to display the condylar tumor more innately. Moreover, computer-assisted surgical simulation and navigation-guided resection of the condylar osteochondroma could be further performed with reference to the three-dimensional digital model of CT images [5–7]. This advantage of CT imaging was unmatched by MRI. In our study, the condylar osteochondromas exhibited varying shapes such as spherical, beak-shaped, hemispherical, pseudopodia, triangular, rectangular, thorn-shaped, oval, lip-like, and cauliflower-like. The adjacent anatomical structures such as the articular eminence, glenoid fossa, articular capsule, maxillary tubercle, and external auditory canal may play a shaping effect on condylar osteochondromas by limiting tumor extension [10, 14].

The continuity of the cortex and medulla of the tumor with the corresponding structures of the parent bone is considered a diagnostic characteristic for osteochondromas [16]. Plain film usually shows this characteristic appearance in lesions of the long bones with standard radiographic projections. However, for osteochondromas occurring in complex areas of anatomy, the continuity may not be apparent on plain radiography. However, CT and MRI with multiple-planar imaging capability often allow optical depiction of the pathognomonic continuity of the lesion and parent bone [2]. This study showed that both CT and MRI could reveal the cortical and marrow continuity of the lesion and the host condyle.

Another important feature of osteochondromas is the hyaline cartilage cap covering the tumor surface. The thickness of the cartilage cap is important to identify malignant transformation of the tumor. CT can show calcified cartilage caps, but it is difficult to identify uncalcified cartilage caps with density similar to the adjacent soft tissue on CT images [2, 17]. As such, MRI is the optimal imaging modality to illustrate the hyaline cartilage cap of osteochondromas. The large water content of the uncalcified cartilage cap provides a very-high signal intensity on T2WI. The cartilage cap has a low-signal intensity in the calcified regions on all pulse sequences of MRI and eventually turns into a yellow bone-marrow signal with the process of ossification [4, 17]. These features allow MRI to differentiate the cartilage cap from the surrounding soft tissues and accurately measure the thickness of the cartilage cap. The current study showed that the detection rate of the cartilage cap with MRI (63.6%) was significantly higher than that with CT (36.4%). The thickness of cartilage cap is related to the degree of skeletal maturity. The thickness of the cartilage cap is generally 1–3 cm in young patients, but only a few millimeters or even completely absent in adults. When the thickness of the cartilage cap is > 2 cm in skeletally mature adults, a malignant transformation into chondrosarcoma is highly suspected [8, 17]. In our study, none of the patients had a cartilage cap thickness of ≥ 2 cm or malignant transformation. When the cartilage cap covering the tumor surface grew thinner or was even missing due to ossification, the condylar osteochondroma could be easily misdiagnosed as condylar hyperplasia.

Histologically, osteochondromas often manifest as a thin layer of fibrous annular perichondrium on the surface of the cartilage cap [18]. The perichondrium has a similar density as the surrounding skeletal muscles, which is difficult to detect on CT. On MR images, the perichondrium manifests as a thin layer of low-signal area surrounding the surface of the cartilage cap. If the underlying cartilage cap shows low-signal intensity due to complete calcification, the presence of the perichondrium will be difficult to detect on MR images [2, 17, 19]. This study showed that MRI had a significantly higher detection rate of the perichondium (45.5%) than CT (6.1%).

Although osteochondroma is benign, it may cause pressure erosion of the adjacent bone tissues due to progressive expansion [17]. The condylar osteochondroma, especially protruding superiorly or expanding extensively, often causes compressive reconstruction of the temporal bone joint surface [10] and even invades the skull base [16]. Eight of the 33 cases in our study showed flattened temporal bone articular surfaces as compared to the opposing side due to the compression of the tumor body. With the condylar osteochondroma gradually growing, especially when extending upward, pseudojoints could be slowly formed between the anterior joint eminence or the middle cranial base and the tumor; further, the affected condyles could dislocate from the glenoid fossa [10]. In our study, there were 12 cases (36.4%) of pseudoarthrosis and 10 cases (30.3%) of condylar dislocation. Among these cases, all tumors were located at the top or in the superior aspect of the condyle.

Osteochondroma may cause alterations in adjacent soft-tissue structures. Buoncristiani *et al*. reported that MRI showed fatty degeneration of the ipsilateral lateral pterygoid muscle in a case of osteochondroma originating from the glenoid fossa [20]. Furthermore, Avinash *et al*. reported that CT images in the soft-tissue window demonstrated fatty infiltration and muscular atrophy of the ipislateral masticator muscle in a case of condylar osteochondroma [3]. Due to excellent soft-tissue resolution, MRI has more advantages over CT with regard to revealing the soft-tissue changes around the tumor. Accordingly, a previous study reported MRI as a reliable method for assessing the presence of muscular atrophy with fatty degeneration [17]. Similarly, our study showed that MRI had a higher detection rate of the affected lateral pterygoid muscle atrophy with fatty infiltration than CT, although the difference was not statistically significant. Muscular atrophy with fatty degeneration might be a functional response of the masticatory muscles to the aberrant mandibular position caused by condylar osteochondroma [20].

The literature includes a few studies on the structural changes of the TMJ in patients with condylar osteochondroma. However, only a few studies on the radiographic presentation of condylar osteochondroma on plain films and CT images analyzed the changes in bone tissues such as reconstruction of the temporal bone joint surface and condylar dislocation [10]. Thus far, there is no report on articular disc displacement and joint effusion. CT did not clearly show the articular disc and joint effusion. However, MRI was considered a gold standard for evaluating the shape and position of the TMJ disc. The display rate of the articular disc by MRI was 100%, and the joint effusion state could also be observed by MRI [21]. Condylar osteochondroma can cause a change in the connection between the articular disc and the condyle. In this study, MRI showed that 4 patients had a disc displacement in the affected side. Of note, the tumor could also cause an articular disc displacement at the contralateral TMJ, and contralateral disc displacement was more common and more complex than disc displacement on the affected side. In this group, 6 patients had articular disc displacement at the contralateral side, including various situations such as reversible anterior displacement, irreversible anterior displacement, reversible medial-anterior displacement, and irreversible lateral-anterior displacement. In addition to the 20 cases of ipsilateral joint effusion, MRI showed that 14 cases of contralateral TMJ had joint effusion. Condylar osteochondroma often leads to a habit of unilateral mastication due to cross-bite on the contralateral side and open bite on the affected side [10, 22]. This might cause changes in the contralateral TMJ structures.

Conclusions

Both CT and MRI clearly demonstrate the characteristic continuity of condylar osteochondroma with the underlying native condylar cortex and medulla as well as changes in the adjacent hard tissue. Three-dimensional reconstruction of CT images could display the tumor's spatial position and morphology more innately than MRI. However, MRI may be superior to CT in revealing the cartilage cap and perichondrium as well as the changes in the TMJ and adjacent soft tissues.

Conflict of interest

The authors indicated no potential conflicts of interest.

References

1. Wilson GJ, Gardner A, Downie J, *et al*. Progressive facial asymmetry resulting from condylar osteochondroma – A case report detailing the resection, subsequent orthognathic intervention and custom joint replacement. J Oral Biol Craniofac Res, 2015, 5: 102–105.
2. Murphey MD, Choi JJ, Kransdorf MJ, *et al*. Imaging of osteochondroma: variants and complications with radiologic-pathologic correlation. Radiographics, 2000, 20: 1407–1434.
3. Avinash KR, Rajagopal KV, Ramakrishnaiah RH, *et al*. Computed tomographic features of mandibular osteochondroma. Dentomaxillofac Radiol, 2007, 36: 434–436.
4. Kim HK, Horn P, Dardzinski BJ, *et al*. T2 Relaxation Time Mapping of the Cartilage Cap of Osteochondromas. Korean J Radiol, 2016, 17: 159–165.
5. Yu HB, Sun H, Li B, *et al*. Endoscope-assisted conservative condylectomy in the treatment of condylar osteochondroma through an intraoral approach. Int J Oral Maxillofac Surg, 2013, 42: 1582–1586.
6. Yu H, Jiao F, Li B, *et al*. Endoscope-assisted conservative condylectomy combined with orthognathic surgery in the treatment of mandibular condylar osteochondroma. J Craniofac Surg, 2014, 25: 1379–1382.
7. Shen ML, Yu JS, Yu HB, *et al*. Establishment and application of a

digital workflow in the treatment of condylar osteochondroma and secondary dentofacial deformities using image-guided endoscopic navigation combined with orthognathic surgery. Chin J Stomatol (Chinese), 2016, 51: 728–733.
8. Bernard SA, Murphey MD, Flemming DJ, *et al*. Improved differentiation of benign osteochondromas from secondary chondrosarcomas with standardized measurement of cartilage cap at CT and MR imaging. Radiology, 2010, 255: 857–865.
9. Muñoz M, Goizueta C, Gil-Díez JL, *et al*. Osteocartilaginous exostosis of the mandibular condyle misdiagnosed as temporomandibular joint dysfunction. Oral Surg Oral Med Oral Pathol Oral Radiol Endod, 1998, 85: 494–495.
10. Meng Q, Chen S, Long X, *et al*. The clinical and radiographic characteristics of condylar osteochondroma. Oral Surg Oral Med Oral Pathol Oral Radiol, 2012, 114: e66–e74.
11. Koga M, Toyofuku S, Nakamura Y, *et al*. Osteochondroma in the mandibular condyle that caused facial asymmetry: a case report. Cranio, 2006, 24: 67–70.
12. Peroz I, Scholman HJ, Hell B. Osteochondroma of the mandibular condyle: a case report. Int J Oral Maxillofac Surg, 2002, 31: 455–456.
13. Huang D, He DM, Yang C, *et al*. Computer-assisted local resection for exostosis osteochondroma of the mandibular condyle. J Craniofac Surg, 2013, 24: e446–e449.
14. Zhang J, Wang H, Li X, *et al*. Osteochondromas of the mandibular condyle: variance in radiographic appearance on panoramic radiographs. Dentomaxillofac Radiol, 2008, 37: 154–160.
15. González-Otero S, Navarro-Cuéllar C, Escrig-de Teigeiro M, *et al*. Osteochondroma of the mandibular condyle: Resection and reconstruction using vertical sliding osteotomy of the mandibular ramus. Med Oral Patol Oral Cir Bucal, 2009, 14: E194–E197.
16. Kim SG, Lim H, Chang CN, *et al*. Jaw deviation and ankylosis caused by condylar osteochondroma: long-term treatment outcome. J Oral Maxillofac Surg, 2014, 72: 604.
17. Woertler K, Lindner N, Gosheger G, *et al*. Osteochondroma: MR imaging of tumor-related complications. Eur Radiol, 2000, 10: 832–840.
18. Lee JK, Yao L, Wirth CR. MR imaging of solitary osteochondromas: report of eight cases. AJR Am J Roentgenol, 1987, 149: 557–560.
19. Sato K, Kodera T, Kitai R, et al. Osteochondroma of the skull base: MRI and histological correlation. Neuroradiology, 1996, 38: 41–43.
20. Buoncristiani RD, Casagrande A, Felsenfeld AL. Osteochondroma of the glenoid fossa: occurrence in an atypical location. J Oral Maxillofac Surg, 2003, 61: 134–137.
21. Tanaka T, Morimoto Y, Masumi S, *et al*. Utility of frequency-selective fat saturation T2-weighted MR images for the detection of joint effusion in the temporomandibular joint. Dentomaxillofac Radiol, 2002, 31: 305–312.
22. Iwata T, Kawata T. Preoperative and postoperative examination of occlusal and maxillofacial changes after osteochondroma extirpation. Am J Orthod Dentofacial Orthop, 2016, 149: 259–268.

DOI 10.1007/s10330-018-0272-2
Cite this article as: Shen ML, Yu HB, Zhu L, *et al*. Comparison of computed tomography and magnetic resonance imaging for the detection of mandibular condylar osteochondroma. Oncol Transl Med, 2018, 4: 108–115.